ELSEVIER

Journal of Immunological Methods 311 (2006) 117 – 129

JIM
Journal of Immunological Methods

www.elsevier.com/locate/jim

Research paper

Quantitative measurement of nuclear translocation events using similarity analysis of multispectral cellular images obtained in flow

Thaddeus C. George [a,*], Stacey L. Fanning [b], Patricia Fitzgeral-Bocarsly [b], Ricardo B. Medeiros [c], Sarah Highfill [c], Yoji Shimizu [c], Brian E. Hall [a], Keith Frost [a], David Basiji [a], William E. Ortyn [a], Philip J. Morrissey [a], David H. Lynch [a]

[a] *Amnis Corporation, 2505 Third Ave., Suite 210, Seattle, WA 98121, USA*
[b] *Graduate School of Biomedical Sciences, University of Medicine and Dentistry of New Jersey, Newark, NJ 07103, USA*
[c] *Department of Laboratory Medicine and Pathology, Center for Immunology, Cancer Center, University of Minnesota Medical School, Minneapolis, MN 55455, USA*

Received 6 September 2005; received in revised form 17 January 2006; accepted 20 January 2006
Available online 10 March 2006

Abstract

Nuclear translocation of NF-κB initiates transcription of numerous genes, many of which are critical to host defense. Fluorescent image-based methods that quantify this event have historically utilized adherent cells with large cytoplasm-to-nuclear area ratios. However, many immunologically relevant cells are naturally non-adherent and have small cytoplasm-to-nuclear area ratios. Using the ImageStream® imaging flow cytometer, we have developed a novel method that measures nuclear translocation in large populations using cross-correlation analysis of nuclear and NF-κB images from each cell. This approach accurately measures NF-κB translocation in cells with small cytoplasmic areas in dose- and time-dependent manners. Further, NF-κB translocation was accurately measured in a subset of cells contained in a mixed population and the technique was successfully employed to measure IRF-7 translocation in plasmacytoid dendritic cells (PDC) obtained from human peripheral blood. The techniques described here provide an objective and statistically robust method for measuring cytoplasmic to nuclear molecular translocation events in a variety of immunologically relevant cell types with characteristically low cytoplasm-to-nuclear area ratios.

Keywords: NF-κB; Signal transduction; Lipopolysaccharide; Image cytometry

1. Introduction

Molecular translocation of transcription factors from the cytoplasm to the nucleus is a pivotal event in many processes critical to cellular activation, differentiation and host defense. Cells of the innate and adaptive immune systems express arrays of receptors, including Toll-like receptors (TLRs), antigen-specific receptors on T cells and B cells, and receptors for a wide variety of both soluble and cell-bound ligands (Janeway and Medzhitov, 1998; Ulevitch and Tobias, 1999; Aderem and Ulevitch, 2000;

Abbreviations: 7-AAD, 7-aminoactinomycin D; BDCA, blood dendritic cell antigen; CCD, charge coupled device; HSV, herpes simplex virus; IDEAS®, ImageStream Data Analysis and Exploration Software; IRF, IFN regulatory factor; LPS, lipopolysaccharide; MOI, multiplicity of infection; NF-κB, nuclear factor κB; PBMC, peripheral blood mononuclear cells; PCC, Pearson's correlation coefficient; PDC, plasmacytoid dendritic cell; PMA, phorbol 12-myristate 13-acetate; PFA, paraformaldehyde; *S*, similarity; TDI, time delay integration; TLR, Toll-like receptor.

* Corresponding author. Tel.: +1 206 576 6859; fax: +1 206 576 6895.
E-mail address: t.george@amnis.com (T.C. George).

0022-1759/$ - see front matter © 2006 Elsevier B.V. All rights reserved.
doi:10.1016/j.jim.2006.01.018

Takeda et al., 2003). Ligand binding initiates intracellular signaling cascades that result in the translocation of transcription factors from the cytoplasm to the nucleus, culminating in the expression of genes involved in host defense. For example, bacterially derived LPS signals nuclear translocation of NF-κB in monocytes, resulting in expression of the pro-inflammatory cytokines TNF-α and IL-κβ (Poltorak et al., 1998; Du et al., 1999; Beutler, 2000). Antigen-specific or mitogen-mediated stimulation of T cells induces NF-κB translocation, followed by proliferation, cytokine secretion and differentiation of effector cell function. Stimulation with enveloped viruses such as Herpes simplex virus (HSV-1) induces nuclear translocation of IRF-7 in circulating human plasmacytoid dendritic cells (PDC), resulting in IFN-α production (Au et al., 1998; Sato et al., 1998; Cella et al., 1999; Siegal et al., 1999; Izaguirre et al., 2003; Dai et al., 2004). In all of these cases, nuclear translocation of a cytoplasmic molecule serves as a critical signal leading to transcription of host defense genes.

Existing methods used to measure nuclear translocation have significant limitations. Biochemical techniques are time-consuming, semi-quantitative in nature and must be performed on relatively pure cell populations. Flow cytometric analysis of phospho-protein-specific staining measures the degree of subunit phosphorylation, but does not determine the intracellular localization of the molecule (Krutzik and Nolan, 2003; Krutzik et al., 2004). Microscopic visualization remains the most direct method for measurement. Recent advancements in imaging instrumentation technology and image processing have enabled the numerical scoring of large populations of cells, bringing statistically robust quantitation of nuclear translocation to this historically time-consuming and subjective process (Deptala et al., 1998). These methods typically rely on adherent cells because they are more adaptable to slides and plates, and their relatively large cytoplasmic to nuclear area ratios facilitate spatial intensity quantitation critical to the translocation measurement. However, many cells, including those of the immune system, are naturally non-adherent and have small cytoplasmic to nuclear area ratios, making them poorly suited for quantitation using established microscopic techniques.

Using the ImageStream® cytometer, a novel technology that produces spatially separated multispectral images of cells in flow, we have developed a new method to make statistically robust nuclear translocation measurements in immunologically relevant cell populations using cross-correlation analysis of fluorescent nuclear and transcription factor images from each object (George et al., 2004). This approach accurately measured translocation in cells with small cytoplasmic areas in a dose- and time-dependent manner, as well as in individual subsets of cells contained in a mixed cell population. The ability to quantify nuclear translocation in flow affords the opportunity to study not only suspension-based cell lines but also populations (and subpopulations) of primary cells that can be found in various physiologic fluids, including peripheral blood.

2. Materials and methods

2.1. Virus and cell lines

THP-1 and Jurkat cell lines were cultured in RPM1 1640 media supplemented with 5% fetal bovine serum, 1 mM sodium pyruvate (Mediatech, Herndon, VA), 100 pM nonessential amino acids, 100 U/ml penicillin, 100 μg/ml streptomycin and 2 mM L-glutamine (Bio-Whittaker, Walkersville, MD) in a humidified atmosphere of 5% CO_2 in air at 37 °C. HSV-1 strain 2931 was originally obtained from C. Lopez, then at Sloan-Kettering Institute (New York, NY).

2.2. Preparation of human PDC from peripheral blood

Studies using cells derived from human peripheral blood were approved by the Institutional Review Board of the New Jersey Medical School. Peripheral blood mononuclear cells (PBMC) were isolated by Ficoll-Hypaque (Lymphoprep; Accurate Chemical and Scientific, Westbury, NY) density centrifugation from fresh heparinized peripheral blood obtained with informed consent from healthy volunteers. The layer containing PBMC was removed and washed twice in Hank's balanced salt solution (HBSS, Life Technologies, Grand Island, NY), followed by low speed centrifugation to remove contaminating platelets. Cells were then resuspended in RPM1 1640 media (Life Technologies) containing 10% FCS, 2 mM L-glutamine, 100 U/ml penicillin, 100 μg/ml streptomycin and 25 mM HEPES. An enriched PDC population was obtained from PBMC by negative immunomagnetic selection using the Human Dendritic Cell Enrichment Kit (StemCell Technologies, Vancouver, BC, Canada). PBMC were washed, suspended in MACS buffer (1 × PBS with 0.5% BSA and 2 mM EDTA) at a concentration of 5×10^7 cells/ml and incubated with StemSep Human Dendritic Cell Enrichment Cocktail (100 μl/ml cells) for 15 min at RT followed by incubation with magnetic colloid (60 μl/ml cells) for an additional 15 min at RT. Cells were washed in MACS buffer and run through a MACS LD negative selection column (Miltenyi Biotec,

Auburn, CA) in a magnetic field (MidiMACS, Miltenyi Biotec). The cellular flow-through was collected and washed twice in HBSS for use as enriched PDC.

2.3. Preparation of murine lymph node cells

Single cell suspensions were prepared from peripheral lymph nodes isolated from C57BL/6 mice and red blood cells were lysed with ACK lysis buffer (0.15 M NH_4Cl, 10 mM $KHCO_3$) for 10 min on ice at a concentration of 3×10^7 cells/ml.

2.4. Activation and immunofluorescent detection of NF-κB nuclear translocation

THP-1 cells in exponential growth phase were treated with the indicated concentrations of LPS (Sigma, St. Louis, MO) for the indicated time points in 25 cm^2 flasks. Cells from control and LPS treatment groups were gently scraped from the flask and washed prior to probing. Murine peripheral lymph node cells were left unstimulated or were stimulated with 200 ng/ml of PMA (Sigma) for 10 min at 37 °C, then washed. Where indicated, cells were stained with 10 μg/ml PE-conjugated anti-CD 14 mAbs (Caltag, Burlingame, CA) in PBS (Cambrex Bio Science, Walkersville, MD) for 10 min. After washing, the cells were fixed in 4% paraformaldehyde (PFA) for 10 min, washed and incubated for 20 min with 10 μg/ml rabbit anti-NFλB p65 polyclonal Abs (Santa Cruz Biotechnology, Santa Cruz, CA) in PBS containing 0.1% Triton X-100/2% FBS for 20 min. The cells were then washed and incubated for 20 min with 7.5 μg/ml FITC-conjugated F $(ab')_2$ donkey anti-rabbit IgG (Jackson ImmunoResearch, West Grove, PA) in PBS/2% FBS for 20 min, then washed and resuspended in 1% PFA with 40 μM 7-AAD (Molecular Probes, Eugene, OR) for 5 min and run directly on the ImageStream. In some experiments, AlexaFluor488-conjugated mouse anti-NF-κB p65 monoclonal Abs (Santa Cruz) were used. The time course translocation reactions were stopped by adding 10% PFA to a final concentration of 1% in the flask prior to harvesting and probing. All fixation and staining reactions were done on ice in the dark at a concentration of 3×10^7 cells/ml. All washes were performed with PBS.

2.5. Activation and immunofluorescent detection of IRF-7 nuclear translocation

For the HSV-mediated IRF-7 translocation studies, PBMC were added back to the enriched PDC to bring cells to 2×10^6 cells/ml per condition. The cells were then stimulated for 3 h at 37 °C, 5% CO_2 with HSV-1 (MOI = l). Cells from control and treated groups were washed in 0.1% BSA/PBS and stained with PE-conjugated anti-BDCA-2 and anti-BDCA-4 monoclonal Abs (Miltenyi Biotec) for 20 min at 4 °C, washed in PBS and stored overnight at 4 °C in 1% PFA. Cells were washed and incubated with 4 μg/ml rabbit anti-human IRF-7 antibody (Santa Cruz) in PBS containing 0.1% Triton X-100 for 30 min at RT. The cells were then washed and stained in PBS with 10 μg/ml AF488-conjugated chicken anti-rabbit IgG (Molecular Probes) for 30 min at RT, washed and resuspended in 1% PFA with 40 μM 7-AAD (Molecular Probes) for 5 min and run on the ImageStream.

2.6. ImageStream data acquisition and analysis

The fluorescence image-based method for quantifying nuclear translocation described here relies on the spectral isolation of NF-κB or IRF-7 images from nuclear images by the ImageStream (George et al., 2004). Cells probed with fluorescently labeled antibody to transcription factor, and 7-AAD are hydrodynamically focused, excited with a 488 nm laser light and imaged on a time delay integration (TDI) CCD camera. Light is passed through a spectral decomposition element that directs different spectral bands to spatially distinct channels on the TDI CCD detector. With this technique, a single cell image is optically decomposed into a set of sub-images, each corresponding to a different color component and each with an identical spatial registry of pixels from channel to channel. Images of fixed cells collected on the ImageStream were analyzed using ImageStream Data Exploration and Analysis Software (IDEAS). Because fluorescent probes have broad emission spectra, spectral compensation is digitally performed on a pixel-by-pixel basis prior to data analysis. After compensation, similarity analysis was done on in-focus single cell images. In-focus single cells were classified based on their small bright field area, high bright field aspect ratio (width to height ratio) and high nuclear contrast (as measured by the gradient max feature). Gradient max measures the magnitude of the largest pixel intensity slope over the whole image and in-focus images with sharp edges at their borders tend to have high max gradient scores.

2.7. Derivation of the similarity score from the Pearson's correlation coefficient

The degree of nuclear translocation can be assessed in a qualitative manner by visually comparing a cell's

nuclear fluorescence image to the pattern of fluorescence produced by the NF-κB label. Nuclear translocation is judged to have occurred if the NF-κB and nuclear fluorescence signals overlap with similar shape. Conversely, if the NF-κB signal surrounds the nucleus, it is judged not to exhibit significant translocation. The similarity score described here is a method of quantitatively performing the same assessment. The similarity score has a high positive value if the NF-κB and nuclear images are alike. In contrast, if the NF-κB and image is dim where the nuclear image is bright, the score has a large negative value. The similarity score is derived from the Pearson's correlation coefficient (PCC, ρ), which is based on a linear regression analysis of pairs of values taken from different data sources. The formula for the PCC is given below,

$$\rho = \frac{\sum_i (x_i - X)(y_i - Y)}{\sqrt{\sum_i (x_i - X)^2 \sum_j (y_j - Y)^2}}$$

where x_i, y_i are the per-pixel intensity values of the two images, and X, Y are the corresponding *mean* intensity values. In the case of translocation analysis, the data sources are the nuclear and NF-κB fluorescence images of the same cell. The data pairs are simply the pixel intensities at the same location in each image. Plotting the pixel intensities of the nuclear image against the transcription factor image reveals an inverse correlation for an untranslocated cell and a positive correlation for a translocated cell. The slope of the linear regression line determines the sign of the coefficient, while the quality of the data's fit to the regression line determines its magnitude. The PCC produces values that range from −1 to 1 but distributions at the extreme values of PCC are compressed. In practice, this means that the PCC can discriminate two cell populations that exhibit modest differences in the degree of translocation, but it assigns similar values to cell populations that are highly translocated (or highly untranslocated) and which may be very distinctive by visual inspection. The similarity score (S) addresses this limitation by transforming the PCC (ρ) using the following formula:

$$\text{Similarity} = \ln\left(\frac{1+\rho}{1-\rho}\right)$$

Like the PCC, S is negative in sign for images that are opposites, positive for identical images and close to zero for uncorrelated images. Unlike PCC, S is unbounded and produces normal distributions over large sets of measurements. As a result, the "dynamic range" of the similarity score is higher and correlates more closely to qualitative judgments of visual distinctiveness.

2.8. Derivation of the NF-κB nuclear to cytoplasmic intensity ratio feature

This feature involves separately integrating pixel intensity within the nuclear and cytoplasmic regions of the NF-κB image. The nuclear region of interest, or 'nuclear mask', was defined by contour segmentation of the 7-AAD image followed by a one pixel erosion to ensure that none of the cytoplasm was included. The 'cytoplasmic mask' was created by subtracting the 7-AAD contour mask from the NF-κB image contour mask. The ratio of the NF-κB integral in the nuclear mask to the NF-κB integral in the cytoplasmic mask was then used to create the feature.

2.9. Statistics

The images of treated populations show that not all cells exhibit a translocation event in response to the treatment. The heterogeneous nature of the samples also indicates that nonparametric statistical tests must be used to determine the statistical significance of small changes. Because the changes in IRF-7/7-AAD similarity scores between Mock and HSV treatments of PDC were small, we used the one-sided Mann–Whitney U rank sum statistical test to determine the significance of these differences. This test is useful for detecting small shifts of known sign between unpaired sample measurements, when the measurements are not expected to be normally distributed. The dose of LPS that induced half-maximal NF-κB translocation (EC_{50}) in THP-1 cells was determined using non-linear regression analysis using the program Prism 4.0 (GraphPad, San Diego, CA).

3. Results

3.1. Quantitative assessment of LPS-induced NF-κB nuclear translocation in a non-adherent cell line

Image-based quantification of nuclear translocation depends in part on image quality of sufficient resolution to distinguish the positional location of NF-κB in relation to the nucleus. Multispectral images of either unstimulated or LPS-stimulated THP-1 cells that have been permeabilized and stained with anti-NF-κB and the DNA intercalating dye 7-AAD were acquired on an ImageStream. Spectrally isolated NF-κB and nuclear images along with their composites from representative unstimulated and LPS-stimulated THP-1 cells are presented in Fig. 1A and B, respectively. Inspection of ImageStream image galleries revealed a distinctly

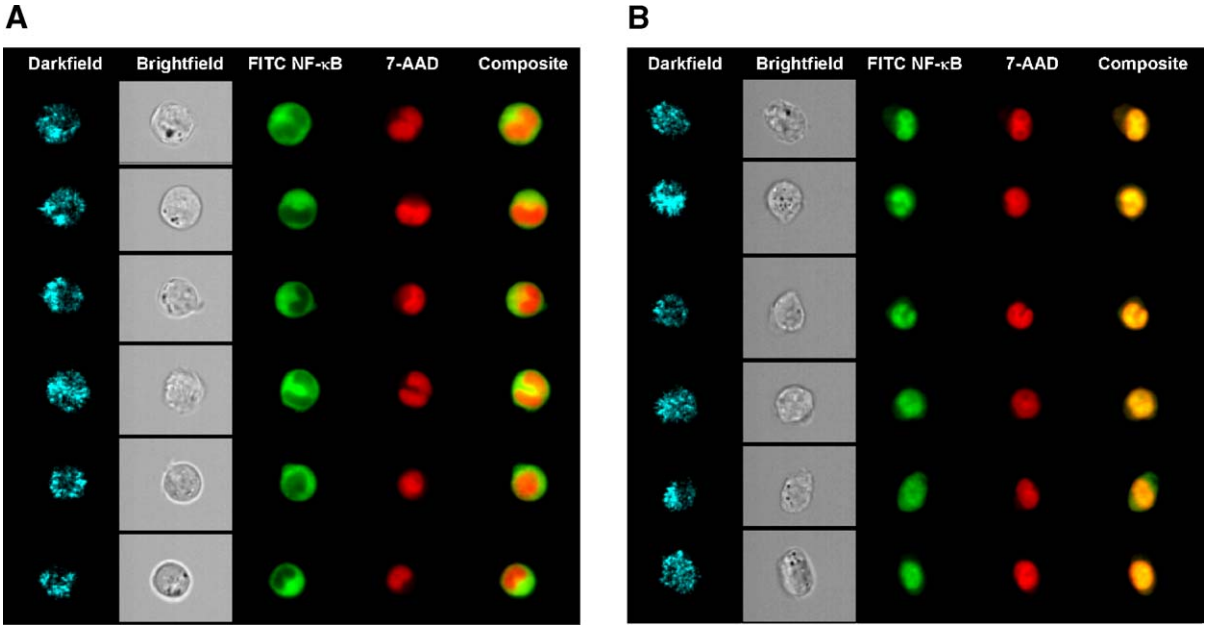

Fig. 1. ImageStream fluorescence imaging of LPS-induced NF-κB nuclear translocation in THP-1 cells. Unstimulated THP-1 cells (A) or THP-1 cells treated with for 1 h with 1 μg/ml LPS (B) were probed for NF-κB expression and 7-AAD as described in Section 2 and run on the ImageStream. Dark field (blue), bright field (white), NF-κB (green), 7-AAD (red) and NF-κB/7-AAD composite images for six representative cells (of 10,000 imaged) are shown for each treatment group.

cytoplasmic distribution of NF-κB in the majority of the unstimulated cells and a nuclear distribution in a majority of the LPS-treated cells.

The relatively large nuclear to cytoplasm ratio and the variable and irregular nuclear shapes of cells belonging to the THP-1 line presented a challenge to image-based quantification of nuclear translocation events. We have developed a measure, called the similarity score (*S*), which is used here to quantify the extent of nuclear translocation in cells that is independent of nuclear shape or cytoplasmic size. The similarity score quantifies the correlation between two spectrally distinct images of a single cell and is derived from the Pearson's correlation coefficient of the pixel intensities of the image pair (see Section 2 for details). The relevant cell images that are used for measuring nuclear translocation are the nuclear image and the NF-κB image. The NF-κB and 7-AAD images from an unstimulated cell (#4762) appear to be inverses of each other, while those images from an LPS-stimulated cell (#1461) closely resemble one another (Fig. 2A). In contrast, the dark field images bear little resemblance to either the NF-κB or 7-AAD images in either cell. Calculation of NF-κB-to-nucleus and NF-κB-to-dark field *S*-values for these two cells is shown graphically in Fig. 2B. The similarity score is calculated for values above a nuclear intensity threshold (represented by the vertical bar) to specifically include all of the nuclear region and the gradient between the nucleus and cytoplasm. The similarity score maps the untranslocated NF-κB/7-AAD inverse image pair to a large negative value (−2.07), the unrelated dark field/7-AAD image pairs to a middle values (−0.17 and −0.19) and the translocated NF-κB/7-AAD image pair to a large positive value (2.82).

Using this analytical approach, we measured the degree of NF-κB nuclear translocation in unstimulated and LPS-stimulated populations of THP-1 cells (more than 5000 events each). An objective method was used to determine the threshold similarity value that identifies translocated cells by analyzing the dark field/7-AAD *S*-values, a scoring that maps uncorrelated imagery (Fig. 2C, left histogram). The positive region (High Sim) on the dark field/7-AAD similarity plot represents the region of 99% confidence that the images positively correlate. This region was applied to the NF-κB/7-AAD similarity histograms of unstimulated and LPS-stimulated THP-1 cells to enumerate translocated cells (Fig. 2C, middle and right histograms, respectively). Using this approach, only 5% of unstimulated cells fell within the 'High Sim' region, indicating that the preponderance of cells in this population exhibited a cytoplasmic NF-κB distribution. In contrast, over 95% of the LPS-stimulated cells fell within the 'High Sim' gate, indicating nuclear translocation of NF-κB.

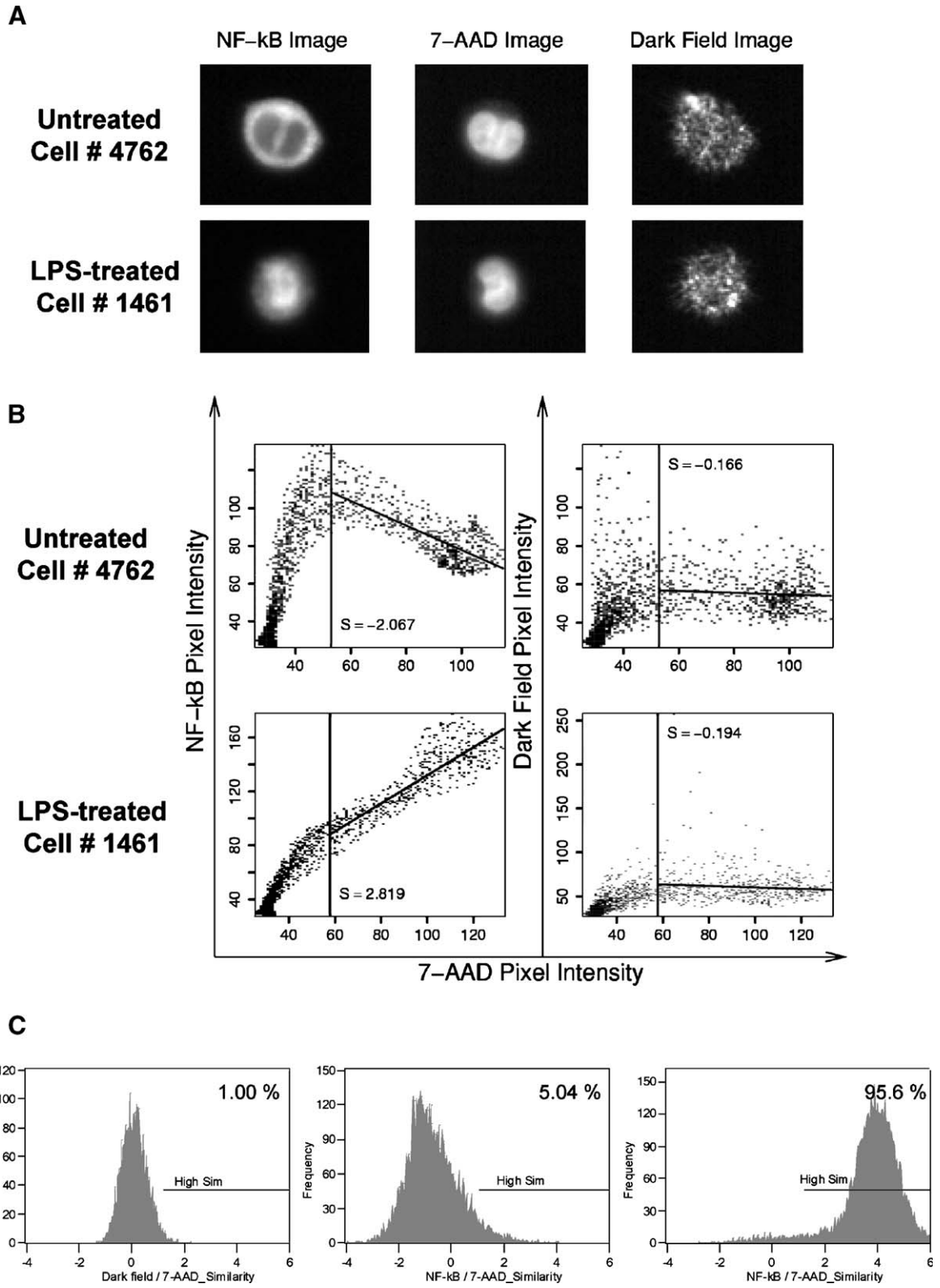
A
NF–kB Image
7–AAD Image
Dark Field Image
Untreated
Cell # 4762
LPS-treated
Cell # 1461
B
Untreated
Cell # 4762
LPS-treated
Cell # 1461
NF–kB Pixel Intensity
Dark Field Pixel Intensity
7–AAD Pixel Intensity
S = –2.067
S = –0.166
S = 2.819
S = –0.194
C
1.00 %
5.04 %
95.6 %
High Sim
Frequency
Dark field / 7-AAD_Similarity
NF-kB / 7-AAD_Similarity

3.2. Comparing the similarity method to nuclear to cytoplasmic intensity ratio method for quantifying nuclear translocation

An established image-based method of quantifying nuclear translocation takes the ratio of nuclear to cytoplasmic-localized NF-κB signal intensity. As NF-κB moves to the nucleus with activation, the nuclear to cytoplasmic intensity ratio is expected to increase. We compared the similarity method to the ratio method (see Section 2) for the ability to measure NF-κB translocation in THP-1 cells (Fig. 3). With LPS treatment, we observed an increase in both scores. Image galleries revealed that cells within the low *S*-value group had cytoplasmic distributions of NF-κB staining, while cells within the high *S*-value population had nuclear-localized NF-κB (Fig. 3C). The key difference noted between the methods was that two populations in the treated group were readily distinguishable using the similarity method but not the ratio method.

3.3. Time course and dose responsiveness of LPS-induced NF-κB nuclear translocation

Activation of THP-1 cells by LPS is known to be both a time- and dose-dependent event. To evaluate the kinetics of NF-κB translocation from the cytoplasm to the nucleus, THP-1 cells were incubated in either medium alone or medium containing LPS (100 ng/ml) for 0, 10, 20, 30, 45, 60 or 90 min, followed by processing and measurement of NF-κB/7-AAD similarity (Fig. 3A). After 10 min of stimulation, only a very low percentage of cells were detected with positive translocation, but this was found to increase rapidly to a maximum level within 45 min (Fig. 4A). No significant differences were observed among cells stimulated for 45, 60 or 90 min. The sensitivity of NF-κB nuclear translocation to LPS stimulation was also measured using this procedure. Cells stimulated for 1 h with concentrations of LPS ranging from 100 pg/ml to 1 mg/ml were stained and analyzed using the ImageStream (Fig. 3B). The results obtained show a sigmoid dose–response curve, with an EC_{50} of 6.31 ng/ml, similar to results obtained elsewhere (Du et al., 1999).

3.4. Quantitation of nuclear translocation in a mixed subpopulation of cells

A potential advantage of ImageStream-based evaluation of nuclear translocation is the ability to detect and quantify this event in discrete subpopulations contained within a larger, heterogeneous population of cells. To test this possibility, we stimulated a mixed population of Jurkat T lymphoma cells and THP-1 cells with LPS for 60 min. Cells were then stained with PE anti-CD14, AlexaFluor488 anti-NF-κB and 7-AAD, and analyzed. THP-1 cells were easily distinguished from Jurkat cells on the basis of positive staining with anti-CD14 (Fig. 5). As expected, no difference in NF-κB association with the nucleus was detected between THP-1 and Jurkat cells that had not been stimulated with LPS. However, in the culture stimulated with LPS a significant increase in both the mean *S*-value and in the percentage of translocated cells was observed in the $CD14^+$ THP-1 cells compared to the unstimulated controls, but not in the $CD14^-$ Jurkat cells. The results of this experiment not only demonstrate that subpopulations of cells in heterogeneous mixtures can be detected and independently analyzed, but also that there was no activation of the Jurkat T cells in the culture system.

3.5. NF-κB nuclear translocation in primary murine cells

The similarity score can theoretically measure nuclear translocation events accurately in cells with low cytoplasm to nuclear area ratios. To test this possibility, we evaluated the utility of this measurement in primary lymphoid cells. Murine lymph node cells were either left untreated or were stimulated with PMA, then stained with FITC anti-NF-κB and 7-AAD. As shown in Fig. 6A, PMA induced significant NF-κB

Fig. 2. Quantification of nuclear translocation using the similarity algorithm. Calculation of the NF-κB/7-AAD similarity score from images (A) of an untreated cell with a cytoplasmic NF-κB distribution (#4762) and an LPS-treated (1 μg/ml for 1 h) cell with a nuclear NF-κB distribution (#1461). Pixel intensities from the 7-AAD images are plotted against the corresponding pixel intensities from the NF-κB or dark field images (B) and the similarity score (*S*) is calculated for those pixels that fall within the region of interest (determined as the pixels whose values for 7-AAD are in the upper 70% of the range and indicated by the vertical line in the plots). Dark field/7-AAD similarity and NF-κB/7-AAD similarity histograms of LPS-treated THP-1 cells (C). The region High Sim drawn on the dark field/7-AAD similarity plot represents the region for positive image correlation for the similarity algorithm. This region is applied to the NF-κB/7-AAD similarity plot. The percentages of cells that fall within High Sim region are displayed in the upper left of each histogram.

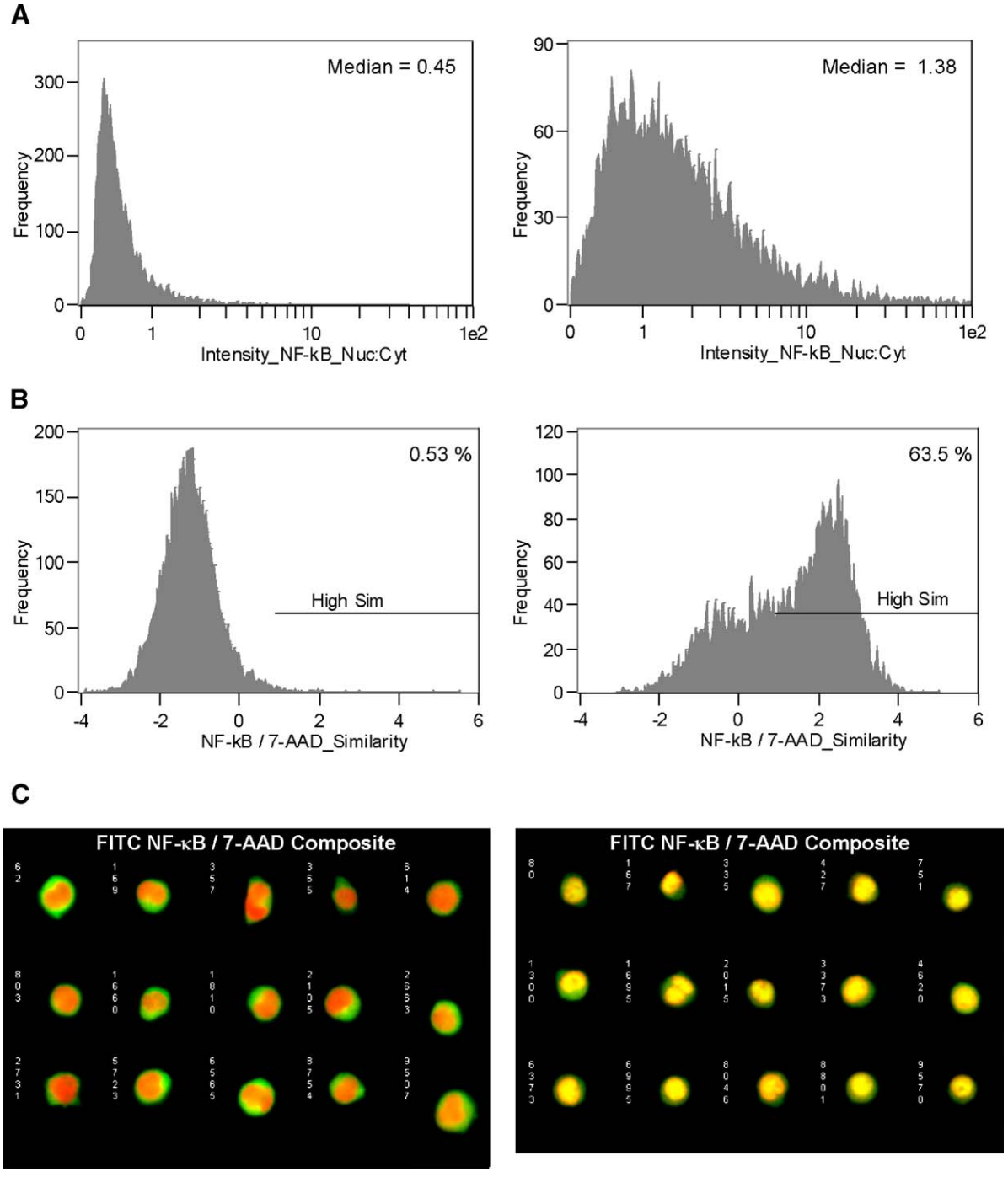

Fig. 3. Comparison of similarity and nuclear/cytoplasmic NF-κB intensity ratio methods for the measurement of NF-κB translocation. NF-κB and 7-AAD images from untreated and LPS-treated (100 ng/ml for 1 h) THP-1 cells were collected on the ImageStream. The ratio of the mean NF-κB image pixel intensity within the nuclear region of the cell to the mean NF-κB pixel intensity within a one-pixel wide cytoplasmic ring (Intensity_NF-κB_Nuc:Cyt) is plotted in (A), while the NF-κB/7-AAD similarity is plotted in (B). NF-κB (green)/7-AAD (red) composite images of representative cells that fall within the High Sim region (right) and to the left of the High Sim region (left) are shown (C).

nuclear translocation as measured by the similarity score (6.49% positive cells in the untreated population vs. 55.3% in the treated population). Representative images from the indicated histogram bins of the treated group demonstrate a distinctly cytoplasmic NF-κB distribution in cells with low *S*-values compared to a nuclear

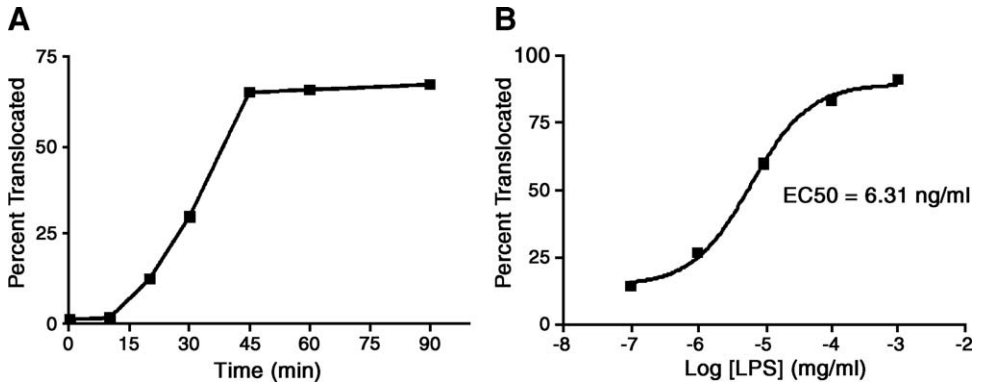

Fig. 4. Time course and dose response of nuclear translocation in THP-1 cells stimulated with LPS. THP-1 cells were cultured with 100 ng/ml LPS for the indicated time points (A), or cultured with the indicated dose of LPS for 1 h (B), probed for NF-κB expression and 7-AAD as described in Section 2 and run on the ImageStream. The percentage of cells with nuclear localized NF-κB (High Sim) was determined for each as described in Fig. 2.

distribution in cells with high scores (Fig. 6B). Thus, the data demonstrate that although a significant proportion of primary lymph node cells responded, not all cells in the treated population had translocated NF-κB in response to PMA at the measured time point.

3.6. IRF-7 nuclear translocation in human PDC

The ability to quantify nuclear translocation in subpopulations of cells and in primary lymphoid cells afforded the possibility of quantifying translocation in

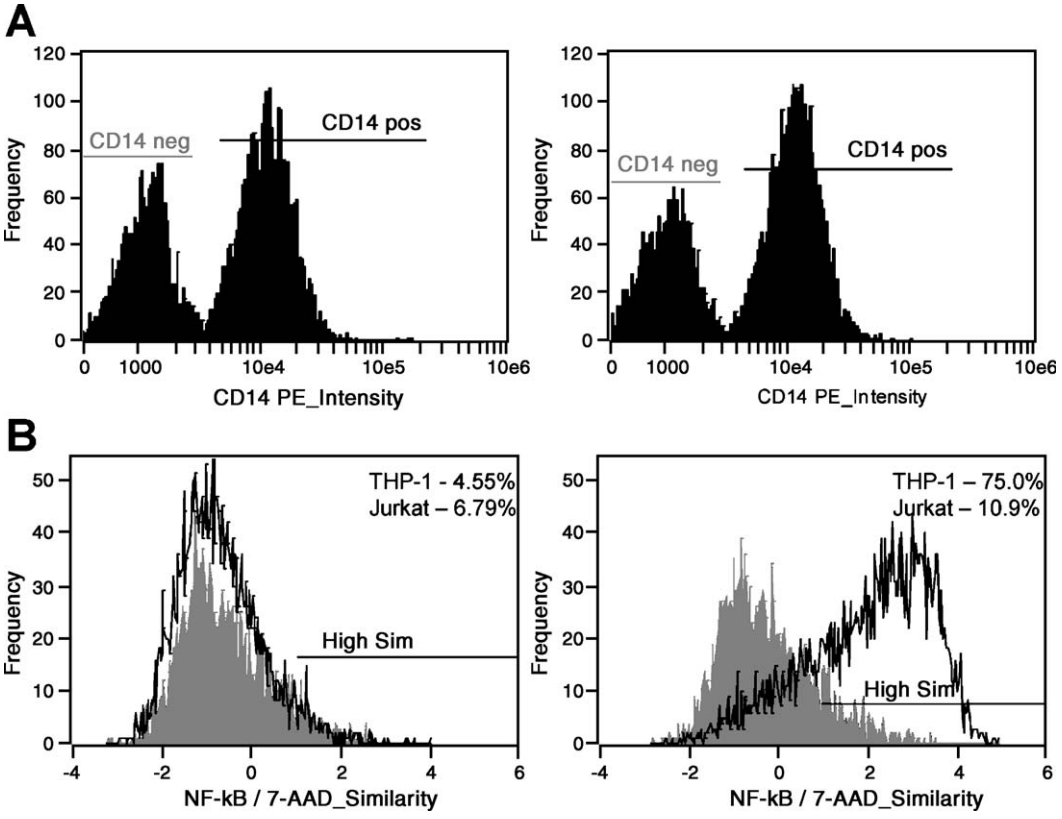

Fig. 5. Detection of nuclear translocation in independent cell subsets within a mixed population. Jurkat (CD14−) and THP-1 (CD14+) cells were identified in co-cultures of cells that were either left untreated (left graphs) or stimulated for 1 h with LPS (right graphs) on the basis of CD14 staining (A). The percentage of CD14+ THP-1 cells (black) and CD14-Jurkat cells (grey) exhibiting nuclear translocation of NF-κB is shown on the NF-κB/7-AAD similarity histogram overlays (B).

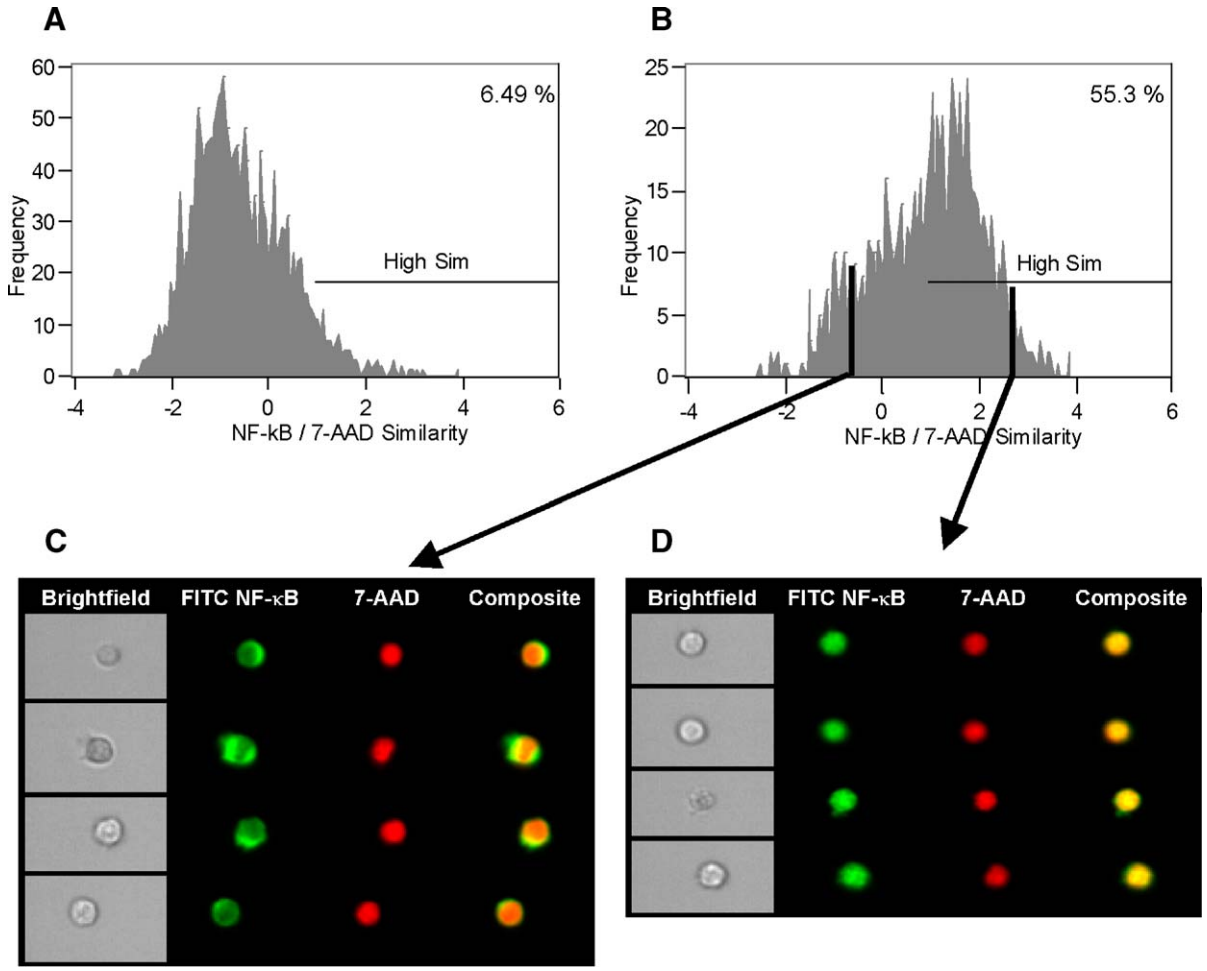

Fig. 6. PMA-induced NF-κB nuclear translocation in primary murine lymph node cells. NF-κB/7-AAD similarity histograms of murine peripheral lymph node cells that were either left unstimulated (A) or were stimulated with PMA (B), then stained for NF-κB expression and 7-AAD as described in Section 2 and run on the ImageStream. The position of the region High Sim was determined as described in Fig. 2C using dark field and 7-AAD images from the unstimulated lymph node sample. Examples of multispectral cell images from the indicated "bins" of the histogram generated from the PMA-treated cells with values of −0.85 (C) and 2.50 (D). Bright field (white), NF-κB (green), 7-AAD (red) and NF-κB/7-AAD (green/red) composite images for each cell are shown.

rare subpopulations of cells contained in human blood. To explore this, we measured the translocation of IRF-7 from the cytoplasm to the nucleus in human peripheral blood PDC following HSV-1 stimulation. Previous studies using standard immunofluorescence microscopy-based techniques demonstrated that a 3 h incubation of human PDC with HSV resulted in visually apparent nuclear translocation of IRF-7 (Dai et al., 2004). Human PDC were left untreated or were stimulated with HSV, stained with fluorescent probes specific for IRF-7, DNA and BDCA-2/4, and imaged on the ImageStream. Multispectral images of PDC were identified on the basis of their IRF-7 bright staining and BDCA-2&4^{+} phenotype (Izaguirre et al., 2003). The percentage of cells with nuclear-localized IRF-7 increased from 3.79% in the unstimulated control sample to 14.9% in the HSV-stimulated sample. Because the differences in *S*-values between the two samples were small both in magnitude and the apparent percentage of PDC that responded to treatment, we employed the one-sided Mann–Whitney *U* rank sum statistical test to determine the significance of these differences. This test demonstrated that the similarity scores were significantly different with a *p*-value <0.0001.

4. Discussion

The study presented here describes a simple and novel method that enables statistically robust quantitation of nuclear translocation events collected in flow in

several cell types. Although microscopic visualization provides compelling evidence of molecular translocation, it can be difficult to analyze large numbers of cells in an objective and repeatable manner, particularly with cell types that have large nuclei and correspondingly thin cytoplasmic regions. Because of these limitations, standard immunofluorescence microscopy remains primarily a qualitative assessment tool used in conjunction with other methods to measure translocation events. Recent advances in imaging technology now allow the rapid collection of large numbers of cell images in flow (George et al., 2004). Combining this technology with a novel application of image similarity analysis, we demonstrate an objective and statistically robust method of quantitating cytoplasmic to nuclear molecular translocation.

Existing image-based methods that quantify translocation rely on intensity measurements of the molecule of interest in the cytoplasmic and nuclear compartments. Relative translocation is typically scored either as the ratio or the difference between the nuclear and cytoplasmic intensities. These approaches require careful spatial determination of these two cellular compartments and are best applied to images with large cytoplasmic to nuclear area ratios (Deptala et al., 1998). The application of these methods to images of small round cells or cells with irregular nuclei is limited due to (1) the difficulty in accurately defining the cytoplasmic compartment for cytoplasmic NF-κB intensity calculations and (2) the high percentage of the total cytoplasmic compartment that resides in front of and behind the nucleus that is included in the nuclear NF-κB intensity calculations as a result of the two-dimensional projection of the cell on the imaging detector. The image similarity method described here has several characteristics that enable statistically robust quantitation of molecular translocation in cells. Because the Pearson's correlation coefficient depends on the relative intensity distribution within the image and not the actual numerical values, the similarity score is insensitive to differences in the pixel intensity dynamic ranges of the images in the image pair. Linear transformation of the pixel intensities of one image relative to another does not change the score. The similarity score is measured within one region of interest that includes all of the nucleus and the intensity gradient between the cytoplasm and the nucleus. No separate cytoplasmic region of interest is determined, simplifying the analytical approach. By quantifying the relative appearance of two images to one another, the similarity method is only influenced by cytoplasmic overlap of the nucleus if the overlap is particularly irregular. Also, because individual cells are isolated in flow, there is no danger that intensity measurements of overlapping cells are included in the analysis. It is important, however, that the region of interest over which the similarity score is calculated not include background or the cell-background boundary region because these image regions will positively correlate in both translocated and untranslocated cells. In practice, the background pixel intensities are far below those containing fluorescence signal, such that automated image segmentation algorithms can repeatedly and objectively determine the boundary between the background and the cell image. These characteristics enabled robust nuclear translocation measurements in cells with irregular nuclear morphology (THP-1) and with very low cytoplasmic to nuclear area ratios (murine lymph node cells, Fig. 6, and PDC, Fig. 7).

The threshold similarity was determined here as the value above which 1% of the dark field and 7-AAD images positively correlate. Because each cell collected on the instrument always has an associated dark field image, this value is readily obtainable for each experiment. In most experimental systems, the median dark field/nuclear image similarity value is near zero with the 95–99% confidence interval close to +1. An advantage to using this method is that it provides an objective means for determining the threshold for each experiment. Alternatively, because the cell images are directly linked to the numerical feature data, the NF-κB/7-AAD similarity threshold can be determined by visual inspection of the associated cell imagery. This allows one to subjectively determine the stringency of the threshold. Once determined, applying the threshold to all files within an experiment provides a suitable nonparametric method for comparing samples data.

The quantitative image-based measurement of IRF-7 nuclear translocation in PDC presented two significant challenges: (1) PDC are infrequent events even in enriched samples and (2) the differences in IRF-7/7-AAD similarity scores between unexposed and HSV-1-stimulated PDC were small. One of the key advantages of high-speed quantitative imaging is the ability to measure morphologic changes in statistically relevant numbers of rare events, and this ability was critically important in determining the significance, using the Mann–Whitney U rank sum test, of the S-value differences observed between the control and HSV-1 groups.

The ability to measure nuclear localization on a per-cell basis for subpopulations within large sample sizes uniquely enabled quantitation of IRF-7 translocation in PDC. Previous studies have shown that IRF-7 is

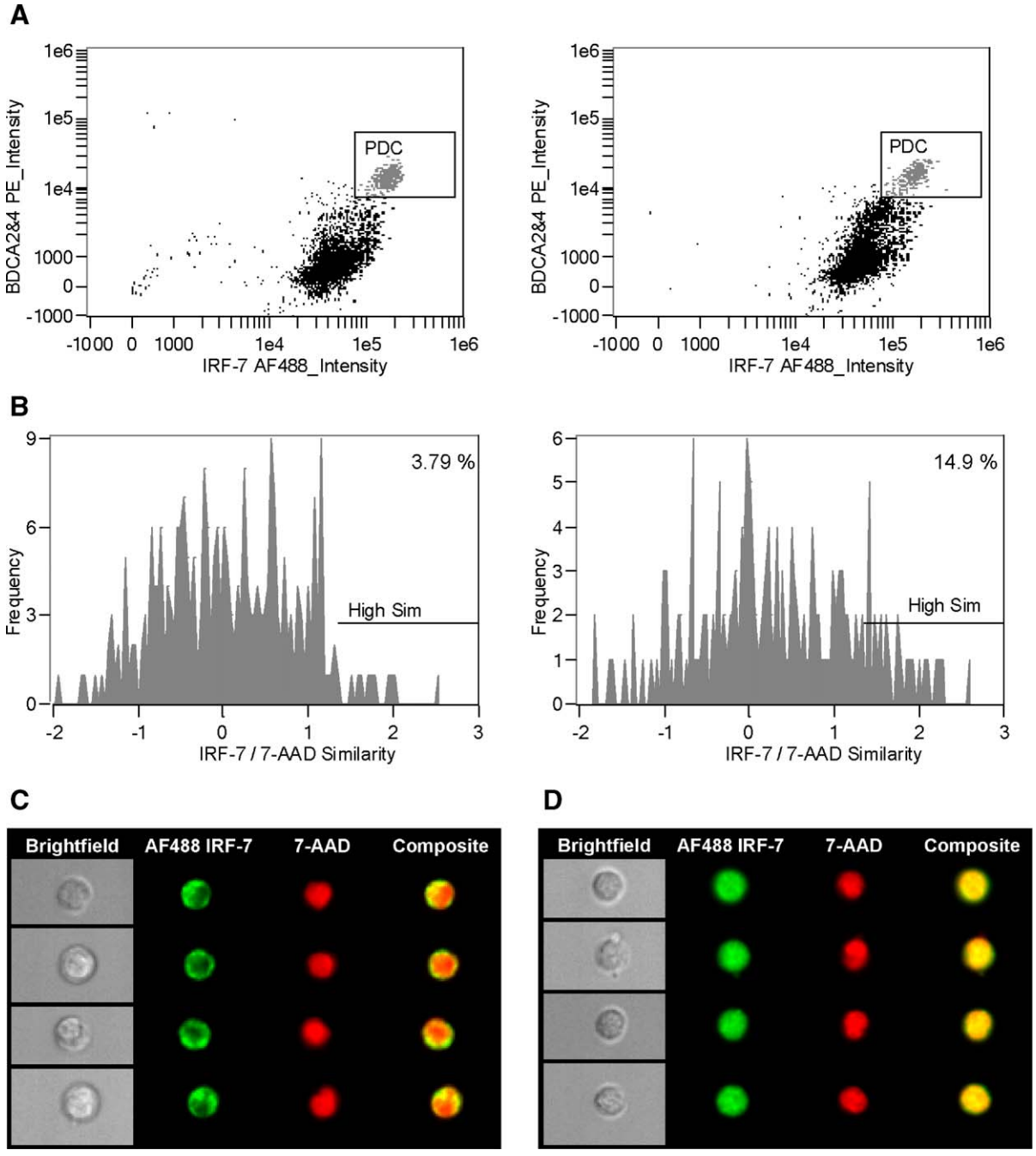

Fig. 7. Measurement of HSV-induced IRF-7 nuclear translocation in human peripheral blood plasmacytoid dendritic cells. PDC from Mock or HSV-stimulated human PBMC were first identified on the basis of BDCA-2/4 positive and bright IRF-7 staining (A), then analyzed for nuclear translocation using the IRF-7/7-AAD similarity score (B). The position of the region High Sim was determined as described in Fig. 2C using dark field and 7-AAD images from the unstimulated PBMC sample. The percentages of PDC in the enriched PBMC and the percentages of PDC with high IRF/7-AAD similarity are shown in the upper left of each plot. This data is representative of three independent experiments.

phosphorylated and translocates to the nucleus in response to viral infection where it induces the expression of many genes, including IFN-α (Au et al., 1998; Marie et al., 1998; Sato et al., 1998; Kumar et al., 2000; Dai et al., 2004). However, routine direct measurement of IRF-7 activation in peripheral blood PDC by traditional Western blot is difficult due to the low numbers of PDC readily obtainable from donors.

Furthermore, Western blot analysis does not provide information about IRF-7 distribution within individual cells. In the study by Dai et al., HSV-induced IRF-7 nuclear translocation was observed in PDC, but the difficulty in manually counting enough cells prevented quantitative analysis. Intracellular staining showed that between 20% and 30% of CD123+ PDC express IFN-α 4 h after HSV infection. Future imaging experiments that simultaneous probe for IRF-7 and LPN-α would allow direct assessment of the relationship between IRF-7 nuclear localization and IFN-α expression in HSV-infected PDC.

In summary, we have demonstrated a method that permits rapid, objective analysis of per-cell nuclear translocation for large numbers of cells in flow. The quantitative method allowed for the sensitive measurement of LPS-mediated NF-κB nuclear translocation in dose response and time course experiments. Combined with immunophenotyping, the independent responsiveness of differentially labeled cell subpopulations to a given stimulus was readily measured in cell lines as well as in primary cell types. Robust quantitation was successfully extended to evaluation of NF-κB translocation in murine lymph node cells with small cytoplasmic compartments. The ability to collect large numbers of images afforded statistically robust measurement of IRF-7 nuclear translocation in rare human peripheral blood PDC.

Acknowledgement

Development of the ImageStream® technology was partially supported by NIH grants 9 R44 CA0l798-02 and 1 R43 GM58956-01.

References

Aderem, A., Ulevitch, R.J., 2000. Toll-like receptors in the induction of the innate immune response. Nature 406, 782.

Au, W.C., Moore, P.A., LaFleur, D.W., Tombal, B., Pitha, P.M., 1998. Characterization of the interferon regulatory factor-7 and its potential role in the transcription activation of interferon A genes. J. Biol. Chem. 273, 29210.

Beutler, B., 2000. T1r4: central component of the sole mammalian LPS sensor. Curr. Opin. Immunol. 12, 20.

Cella, M., Jarrossay, D., Facchetti, F., Alebardi, O., Nakajima, H., Lanzavecchia, A., Colonna, M., 1999. Plasmacytoid monocytes migrate to inflamed lymph nodes and produce large amounts of type I interferon. Nat. Med. 5, 919.

Dai, J., Megjugorac, N.J., Amrute, S.B., Fitzgerald-Bocarsly, P., 2004. Regulation of IFN regulatory factor-7 and IFN-alpha production by enveloped virus and lipopolysaccharide in human plasmacytoid dendritic cells. J. Immunol. 173, 1535.

Deptala, A., Bedner, E., Gorczyca, W., Darzynkiewicz, Z., 1998. Activation of nuclear factor kappa B (NF-kappaB) assayed by laser scanning cytometry (LSC). Cytometry 33, 376.

Du, X., Poltorak, A., Silva, M., Beutler, B., 1999. Analysis of Tlr4-mediated LPS signal transduction in macrophages by mutational modification of the receptor. Blood Cells Mol. Diseases 25, 328.

George, T.C., Basiji, D.A., Hall, B.E., Lynch, D.H., Ortyn, W.E., Perry, D.J., Seo, M.J., Zimmerman, C.A., Morrissey, P.J., 2004. Distinguishing modes of cell death using the ImageStream multispectral imaging flow cytometer. Cytometry A 59, 237.

Izaguirre, A., Barnes, B.J., Amrute, S., Yeow, W.S., Megjugorac, N., Dai, J., Feng, D., Chung, E., Pitha, P.M., Fitzgerald-Bocarsly, P., 2003. Comparative analysis of IRF and IFN-alpha expression in human plasmacytoid and monocyte-derived dendritic cells. J. Leukocyte Biol. 74, 1125 (Electronic publication 2003 Sep 2).

Janeway Jr., C.A., Medzhitov, R., 1998. Introduction: the role of innate immunity in the adaptive immune response. Semin. Immunol. 10, 349.

Krutzik, P.O., Nolan, G.P., 2003. Intracellular phospho-protein staining techniques for flow cytometry: monitoring single cell signaling events. Cytometry 55A, 61.

Krutzik, P.O., Irish, J.M., Nolan, G.P., Perez, O.D., 2004. Analysis of protein phosphorylation and cellular signaling events by flow cytometry: techniques and clinical applications intracellular phospho-protein staining techniques for flow cytometry: monitoring single cell signaling events. Clin. Immunol. 110, 206.

Kumar, K.P., McBride, K.M., Weaver, B.K., Dingwall, C., Reich, N. C., 2000. Regulated nuclear-cytoplasmic localization of interferon regulatory factor 3, a subunit of double-stranded RNA-activated factor 1. Mol. Cell. Biol. 20, 4159.

Marie, I., Durbin, J.E., Levy, D.E., 1998. Differential viral induction of distinct interferon-alpha genes by positive feedback through interferon regulatory factor- 7. EMBO J. 17, 6660.

Poltorak, A., He, X., Smimova, I., Liu, M.Y., Van Huffel, C., Du, X., Birdwell, D., Alejos, E., Silva, M., Galanos, C., Freudenberg, M., Ricciardi-Castagnoli, P., Layton, B., Beutler, B., 1998. Defective LPS signaling in C3H/HeJ and C57BWlOScCr mice: mutations in Tlr4 gene. Science 282, 2085.

Sato, M., Hata, N., Asagiri, M., Nakaya, T., Taniguchi, T., Tanaka, N., 1998. Positive feedback regulation of type I IFN genes by the IFN-inducible transcription factor IRF-7. FEBS Lett. 441, 106.

Siegal, F.P., Kadowaki, N., Shodell, M., Fitzgerald-Bocarsly, P.A., Shah, K., Ho, S., Antonenko, S., Liu, Y.G., 1999. The nature of the principal type 1 interferon-producing cells in human blood. Science 284, 1835.

Takeda, K., Kaisho, T., Akira, S., 2003. Toll-like receptors. Annu. Rev. Immunol. 21, 335 (Electronic publication 2001 Dec 19).

Ulevitch, R.J., Tobias, P.S., 1999. Recognition of gram-negative bacteria and endotoxin by the innate immune system. Curr. Opin. Immunol. 11, 19.